

# Journal of Biomedical Optics

[SPIEDigitalLibrary.org/jbo](http://SPIEDigitalLibrary.org/jbo)

## **Use of Raman spectroscopy in the analysis of nickel allergy**

Javier Alda  
Claudio Castillo-Martinez  
Rodrigo Valdes-Rodriguez  
Diana Hernández-Blanco  
Benjamin Moncada  
Francisco J. González

# Use of Raman spectroscopy in the analysis of nickel allergy

Javier Alda,<sup>a</sup> Claudio Castillo-Martinez,<sup>b</sup> Rodrigo Valdes-Rodriguez,<sup>b</sup> Diana Hernández-Blanco,<sup>b</sup> Benjamin Moncada,<sup>b</sup> and Francisco J. González<sup>c</sup>

<sup>a</sup>University Complutense of Madrid, Applied Optics Complutense Group, Madrid, Spain

<sup>b</sup>Universidad Autónoma de San Luis Potosí, Hospital Central 'Dr Ignacio Morones Prieto, Dermatology Department, SLP, México

<sup>c</sup>Universidad Autónoma de San Luis Potosí, Coordinación para la Innovación y la Aplicación de la Ciencia y la Tecnología, San Luis Potosí, Mexico

**Abstract.** Raman spectra of the skin of subjects with nickel allergy are analyzed and compared to the spectra of healthy subjects to detect possible biochemical differences in the structure of the skin that could help diagnose metal allergies in a noninvasive manner. Results show differences between the two groups of Raman spectra. These spectral differences can be classified using principal component analysis. Based on these findings, a novel computational technique to make a fast evaluation and classification of the Raman spectra of the skin is presented and proposed as a noninvasive technique for the detection of nickel allergy. © 2013 Society of Photo-Optical Instrumentation Engineers (SPIE). [DOI: 10.1117/1.JBO.18.6.061206]

Keywords: Raman spectroscopy; principal component analysis; nickel allergy; dermatology; noninvasive diagnosis.

Paper 12422SS received Jul. 4, 2012; revised manuscript received Oct. 10, 2012; accepted for publication Oct. 12, 2012; published online Nov. 2, 2012.

## 1 Introduction

Metal allergy usually develops following repeated or prolonged skin contact with metal ions. These ions need to get in contact with the epidermis to trigger an allergic response.<sup>1</sup> Even though metal allergy is mainly an environmental disorder, null mutations in the filaggrin gene complex were recently found to be associated with nickel allergy and dermatitis.<sup>1</sup> Filaggrin is a key protein of the epidermis that plays an essential role in the formation of the protective skin barrier. Filaggrin is cross-linked to the cornified cell envelope, which constitutes an insoluble barrier in the stratum corneum, protecting the organism against environmental agents and preventing epidermal water loss.<sup>2</sup> Because filaggrin gene mutations affect the integrity of the stratum corneum, these mutations allow the permeation of metal ions favoring allergic reactions.<sup>1</sup>

Nickel is a common allergen on patch testing in Western countries, affecting 10% of women and 1% to 2% of men. Women are thought to be sensitized through ear piercing and the wearing of nickel-releasing costume jewelry. Nickel allergy is important because of its relationship with vesicular hand dermatitis.<sup>3</sup>

Raman spectroscopy is a vibrational spectroscopy technique in which a laser is focused onto a sample. The interaction of the incident photons with the molecules of the sample generates inelastic scattering of photons with frequencies and intensities characteristic of the molecules in the sample. The resulting Raman spectrum provides a characteristic fingerprint of the molecular composition of the sample.<sup>4</sup> Raman spectroscopy is noninvasive and nondestructive, allowing the analysis of live cells or tissues without perturbation of the sample. It is also worth noting that water is not Raman active, making Raman spectroscopy ideal for biomedical applications.<sup>5,6</sup>

The application of Raman spectroscopy in the field of dermatology dates back to 1992, when the first Raman spectrum of human skin was published.<sup>7</sup> Since then, the use of Raman spectroscopy in the skin has been diversified from characterization of skin components<sup>8</sup> to many other uses such as percutaneous skin absorption of drugs and metabolism of active ingredients,<sup>9,10</sup> interaction of water with other skin cell compounds,<sup>11,12</sup> and medical diagnosis.<sup>13,14</sup>

Raman spectroscopy was proven useful in the noninvasive detection of filaggrin-related atopic dermatitis<sup>15</sup> and filaggrin gene null mutations,<sup>16</sup> which also have been associated with nickel allergy.<sup>1</sup> Besides the obvious lack of filaggrin in the stratum corneum of people with filaggrin gene null mutations, Mlitz et al.<sup>17</sup> found using Raman spectroscopy that the stratum corneum of atopic dermatitis patients with filaggrin gene mutations contained less water, ornithine, urocanic acid, and total natural moisturizing factor than the stratum corneum of healthy controls. Interestingly enough, the patients with atopic dermatitis that did not have filaggrin gene mutations differed significantly from the healthy controls only in the urocanic acid content of the stratum corneum.<sup>17</sup> Because nickel allergy has been related to filaggrin gene mutations,<sup>1</sup> it is possible that the biochemical composition of nickel allergy patients is different from that of healthy subjects.

In this work, the Raman spectra of skin of subjects with nickel allergy is analyzed and compared to the spectra of skin of healthy subjects to detect possible biochemical differences in the structure of the skin and develop a noninvasive method to diagnose metal allergies. This analysis has been carried out by using principal component analysis (PCA). This technique was successfully applied in previous skin studies.<sup>15</sup> The obtained results are analyzed to provide a method to classify the spectra in the two groups, allergic and nonallergic. A typical PCA classification procedure requires a new PCA calculation when new data is included. This calculation depends on the characteristics of the data under analysis and can be

Address all correspondence to: Francisco J. González, Coordinación para la Innovación y la Aplicación de la Ciencia y la Tecnología, Universidad Autónoma de San Luis Potosí, Sierra Leona 550, Lomas 2da. Sección, 78210, San Luis Potosí, México. Tel: +52 (444) 825-0183 ext 232; Fax: +52 (444) 825-0198; E-mail: javier.gonzalez@uaslp.mx

computationally complex. The method presented in this paper calculates the projection of the new data on a selected set of principal components (PCs). This procedure does not need the spectrum under analysis to be included in a new PCA calculation.

## 2 Materials and Methods

Fifteen healthy subjects (11 female and 4 male) participated in this study (median age 23.6 years, SD 3.7, range 21–34). They had no history of any type of skin allergies and no ongoing dermatitis or skin lesions on their hands or arms. A single patch test of nickel sulfate hexahydrate (Chemotechnique Diagnostics, Modemgatan 9, SE-235 39 Vellinge, Sweden) using Finn chambers was applied on the skin of the left forearm to exclude them from allergic contact dermatitis. Also, 10 patients (9 female, 1 male, median age 29.5 years, SD 9.6, range 18–50) with confirmed diagnosis of skin allergic contact dermatitis to nickel with positive patch test (++) allergic reaction according to the International Contact Dermatitis Research Group classification<sup>18</sup>) participated in this study. Patients were free of skin lesions and did not take any oral medications 1 month before the study, and no topical agents were applied to their skin for at least 1 week before the study.

Raman spectra were measured on the skin of both groups. Figure 1 shows the Raman spectra measured for healthy and allergic patients. Measurements were performed on the left arm on the upper volar arm region, 5 cm below the armpit, at room temperature using a Raman Systems R3000 spectrometer (Ocean Optics, Dunedin, FL) with a 785-nm laser diode, a spectral resolution of  $8\text{ cm}^{-1}$ , and a laser power of 90 mW. The measurements were taken with a fiber-optic probe with a spacer in direct contact with the skin so that the focus of the laser beam was right on the skin surface. The acquisition time was set to 1 s, and the average of three spectra was taken as the final measurement. The irradiance of the laser diode used is below the ANSI standard for skin, and none of the participants reported any kind of discomfort when the measurements were performed. The measurements were performed in the  $200\text{ to }1800\text{ cm}^{-1}$  spectral range, and the instrument was calibrated using a Teflon standard every day before each round of measurements. All the measured

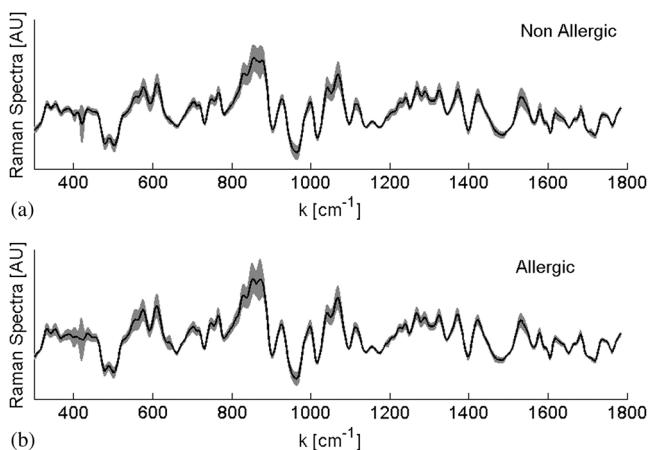


**Fig. 1** Raman spectra of all the patients, divided by (a) nonallergic and (b) allergic. For each group, the solid line corresponds to the mean of the spectra of each group, and the shadow around this line represents the standard deviation at each wavenumber.

spectra were preprocessed by subtracting a fifth-order polynomial to the raw spectra applying the fluorescence removal algorithm proposed by Zhao et al.,<sup>19</sup> also known as the Vancouver Raman algorithm.

The spectra were analyzed using the multivariate technique of PCA.<sup>20</sup> This method provides a collection of pseudo-spectra: the principal components. These PCs are uncorrelated and explain the variance of the data in decreasing order. A rotation matrix describes the transformation from the original data to the principal components. The elements of this rotation matrix can be interpreted as eigenvectors. The variance contributed by each principal component is given by the so-called associated eigenvalue. Taking into account the inherent uncertainty of the set of data, it is possible to determine the uncertainty of the eigenvalues (see appendix A of Ref. 21). When the uncertainties of consecutive eigenvalues overlap, we can group together those eigenvalues connected by their overlapping uncertainties. These eigenvalues define the concept of process.<sup>21,22</sup> Considering another statistical realization of the same phenomenon, i.e., taking again the spectral data under the same experimental conditions, the eigenvectors within a multi-eigenvalue process could be different, but the subspace generated by them will be the same. In some areas, these processes can be linked to physical constraints or measurement conditions. On the other hand, if the uncertainty of an eigenvalue does not overlap with its neighbors, then the process contains one eigenvalue and it will be denoted as a single-eigenvalue process. After applying the PCA method, the number of PCs generated is the same as the original number of spectra. However, since each principal component represents a different amount of variance of the data, this method is typically used to reduce the dimensionality of the data set. The definition of processes will help to make this dimensionality reduction. In the analysis of Raman spectra, we have found that the relevant PCs are those that cannot be connected with any other and that have a large contribution to the total variance of the data set. Therefore, we will focus our attention on the single-eigenvalue processes.

## 3 Results

We begin analyzing the eigenvalues obtained from the PCA, which are usually better represented as relative weights, just by normalizing them to the total variance of the data. The eigenvalues (or weights) are arranged in decreasing order of their contribution to the total variance. The same can be said for the associated PCs. Besides, the grouping mechanism applied to the set of eigenvalues identifies those being independent (single-eigenvalue processes) from a statistical point of view.<sup>21</sup> Figure 2 shows the relative weight for each calculated PC. The filled circles are those that are considered as independent using 99.9% level of confidence.

Figure 3 shows a spectral representation of the principal components belonging to single-eigenvalue processes. Now we look for a combination of them that allows an easy and reliable identification of the two groups: allergic and nonallergic individuals. This search uses the components of the eigenvectors. Eigenvectors are arranged as a square matrix having as many rows and columns as number of spectra. This matrix is the rotation matrix connecting the original spectra with the principal components. Eigenvectors contain the coefficients of the linear combination of principal components that reconstruct any particular spectrum. Also, for a given principal component,

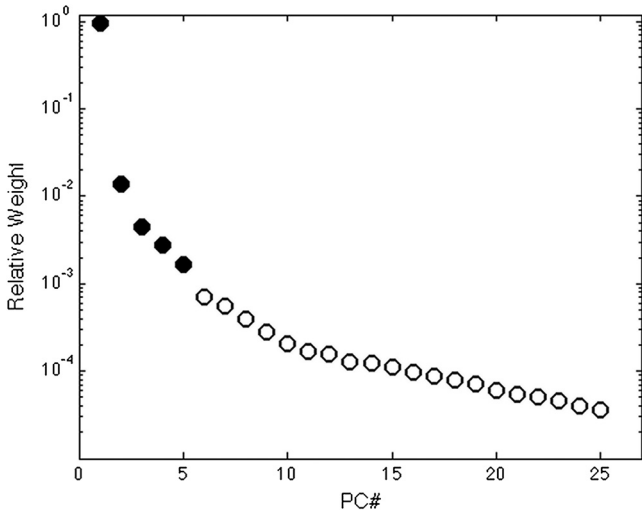


**Fig. 2** Relative weight of the 25 principal components obtained from the original spectra. The solid circles are the first independent principal components, with a 99.9% level of confidence.

they describe the contribution of that principal component in every original spectrum.

After analyzing the 10 possible combinations of the first five eigenvectors taken two at a time, we found that eigenvectors 3 and 5 can be used to distinguish the two groups of patients (see Fig. 4). In Fig. 4, we can see how the patients who show a positive reaction to nickel (dark circles) can be grouped together in a region separated from the location of the patients with a negative reaction to nickel (white circles). The numbers within the symbols are the ID numbers of the patients. The solid line represents an approximate boundary between the two groups. The parameters of this line are obtained by using an optimization process that minimizes a potential function that is inversely proportional to the distance of the points to the boundary line. This optimization also maintains both types of circles separated by the line.

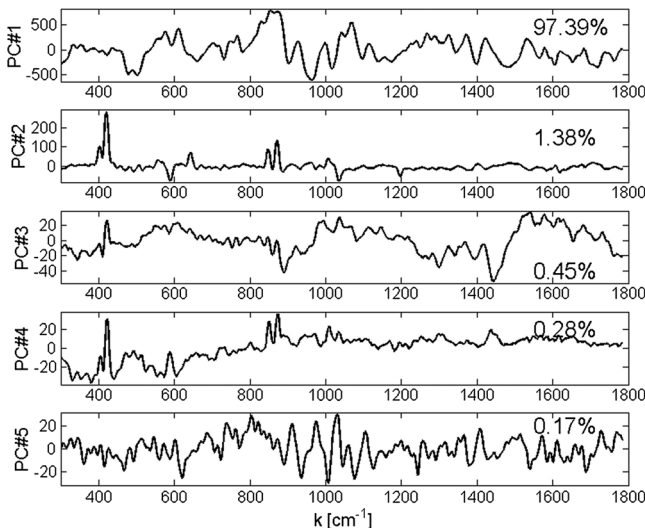


**Fig. 3** Spectra of the five principal components (PCs) that are considered and identified as statistically independent. The numbers within the plot correspond to their relative weights.

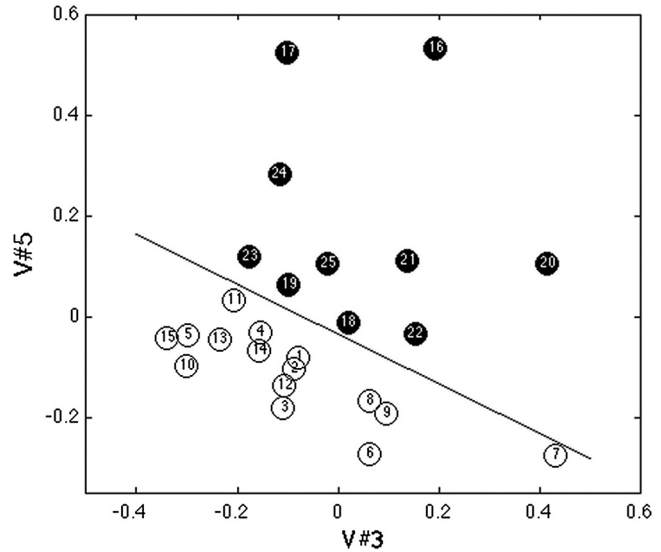


**Fig. 4** Distribution of the components of eigenvectors 3 and 5. The number within the symbol denotes the ID number of the patient. The dark and white circles represent those patients showing allergic reactions and nonallergic reactions, respectively.

This approach is a particular application of the minimum-link red-blue separation problem.<sup>23</sup>

In Fig. 5, we plot principal components 3 and 5. From the previous analysis, these PCs contain the information regarding nickel allergy, and they can be used to partially reconstruct, or filter, all the original data. After performing this reconstruction, and before adding the mean value of the spectrum that was previously subtracted to apply the PCA method, we have made an analysis to locate those wavenumbers where the spectra of the negative and positive reaction groups behave differently; this can give us a method of classification for healthy and allergic individuals. Those wavenumbers are marked in Fig. 5 as grey vertical lines. At those wavenumbers, the reconstructed spectra of all the patients of a given (positive or negative allergic reaction) group is above, or below, the other group's spectra. This is shown for three of those regions in Fig. 6. In this figure, we show how the reconstructed spectra of all patients evolve in these selected regions. The spectra from the patients with negative reaction are all above (first region from 430 to 475  $\text{cm}^{-1}$ ) or below (second and third regions, from 670 to 700 and 1710 to 1735  $\text{cm}^{-1}$ , respectively) the spectra of the patients with a

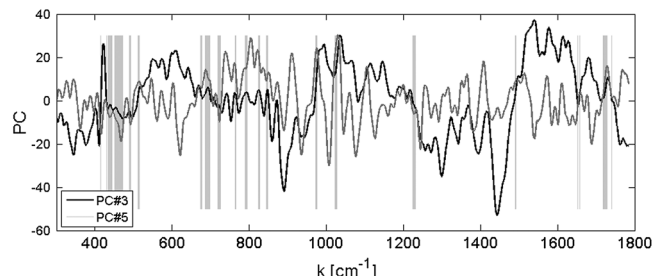


**Fig. 5** Spectral representation of principal components 3 and 5. The vertical lines denote those wavenumbers where the spectra reconstructed with these principal components allows a clear identification of the positive and negative reaction groups.

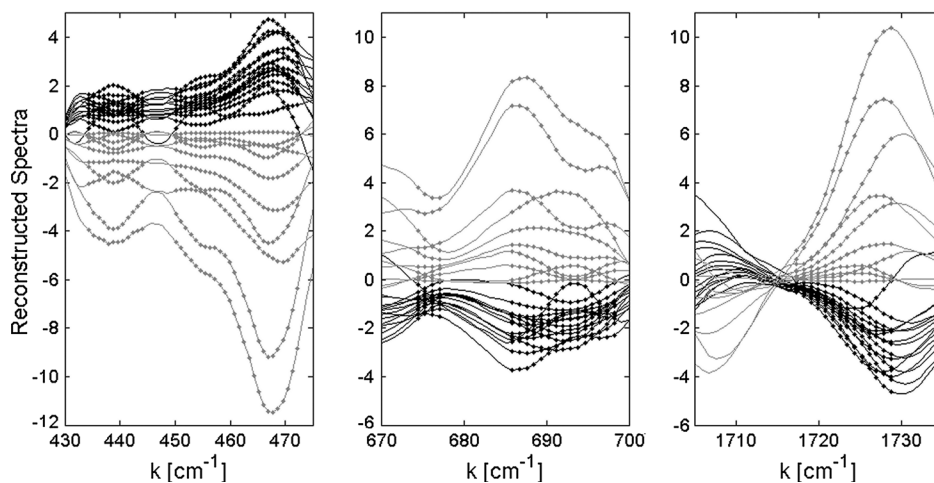


**Fig. 6** Detail of the reconstructed spectra of all patients when using PC 3 and PC 5. In the spectral region from 430 to 475  $\text{cm}^{-1}$  (left), all the patients showing an allergic reaction (in black) have reconstructed spectra below those spectra of the other group (in gray). For the other two spectral regions (center and right), the allergic group has reconstructed spectra above the other group's spectra. The dots are located at those wavenumbers where both groups are clearly separated from each other.

positive reaction to nickel. The dots in the graph indicate the spectral wavenumbers different for the two groups. The results of this spectral analysis may help researchers to focus on specific spectral regions to find special characteristics of the skin molecules playing a decisive role in the development of allergic reactions.

Because the method previously used relies on performing the PCA on all the data, if a new spectrum needs to be analyzed then the whole analysis needs to be repeated with the new set of data. To provide a tool for a fast evaluation and reliable classification of a given spectra into the two clinically different groups, a new methodology is proposed in this work. First we evaluate the dot product, or score, of the spectrum under analysis times the principal components 3 and 5. These two values represent the cosine between the original spectra and the selected principal components. To obtain these parameters, the mean value of the spectrum of the patient needs to be subtracted from the original one, and the following equation is evaluated:

$$C_{j,\text{patient}} = \frac{\int S_j(k)S_{\text{patient}}(k)dk}{\sqrt{\int [S_j(k)]^2 dk} \sqrt{\int [S_{\text{patient}}(k)]^2 dk}}, \quad (1)$$

where  $S_j$  and  $S_{\text{patient}}$  are the spectra of the principal component  $j$  and the patient (after removing the mean of the spectrum), respectively. Our new approach consists in calculating  $C_{3,\text{patient}}$  and  $C_{5,\text{patient}}$ . Alternatively, Eq. (1) can be interpreted as a scaled version of scores 3 and 5 of the spectrum of the patient. The results of this calculation for the spectra used in this study are shown in Fig. 7. Since we are using the same set of data, the resulting figure is similar to Fig. 4, in which the components of the eigenvalues 3 and 5 were plotted. Again, it is easy to distinguish the two groups by just tracing a line separating the location of these parameters. The parameters of the line are obtained through an automatic procedure. Actually, this division line is the main result of this analysis. The location of the calculated parameter for a given patient spectrum below or above this line will classify the patient as healthy or allergic. The main advantage of this calculation over the evaluation of the components of eigenvectors is that it can be applied to any Raman spectra without the need of a new PCA evaluation

involving the new spectrum under analysis. On the other hand, the reliability of the method lies in the quality of the spectral database used to obtain the principal components used to set the dividing line.

To prove the validity and reliability of the proposed method, we have performed a leave-one-out cross-validation (LOOCV) technique.<sup>24</sup> As we have 25 spectra, we have performed 25 PCA calculations. Each one of them leaves one of the patients out and calculates the principal components. Because we left one spectrum out of the calculation, we obtain 24 principal components. Then, the parameter defined in Eq. (1) is calculated for each patient for principal components 3 and 5. Figure 8 shows the results of this test. We have represented as open circles the values obtained in our previous calculation with all spectra, and also presented in Fig. 7. The thick line obtained previously is also represented and separates the two types of patients. The

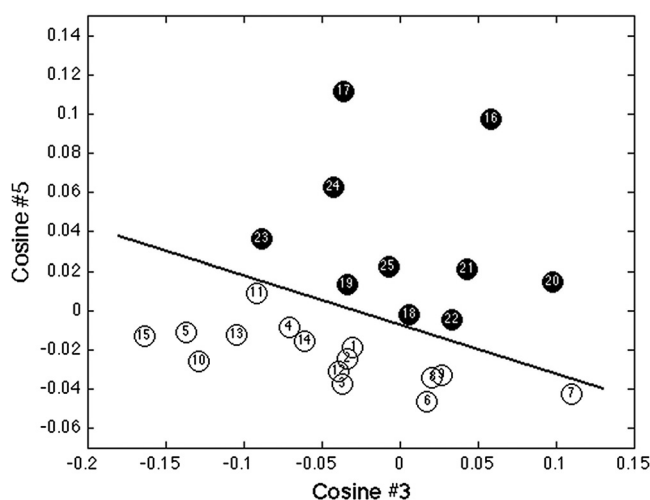


**Fig. 7** Map of the cosines for each one of the spectra in the original data. These cosines are calculated for principal components 3 and 5. The solid line separates the locations of the spectra of the allergic and nonallergic groups. The dark circles represent those patients showing allergic reaction. The white circles denote the patients that do not show an allergic reaction.

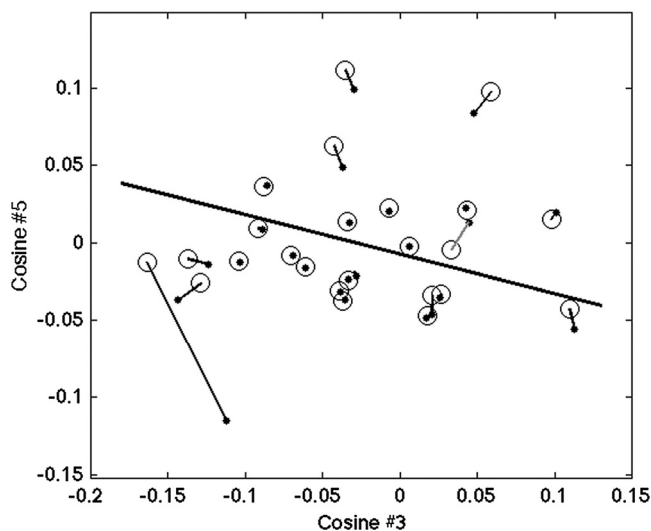


**Fig. 8** Representation of the effect of applying the LOOCV test to the spectra. The white circles are located at the same point presented in Fig. 7 and are obtained from principal component analysis (PCA) with the 25 patients. The dots are the locations for the patients, when each patient is left out and the PCA is obtained using the other 24 spectra. We have also represented the line connecting both locations for each patient. The location of patient 22 is obtained considering PC 4 instead of PC 5. This change is justified after comparing PC 4 for this case with PC 5 for the rest of the patients. We have plotted this case in gray.

dots are the locations for each patient when calculating  $C_{3,\text{patient}}$  and  $C_{5,\text{patient}}$  of the patient left out. The thin line connects the two locations for the same patient. Although some of the patient's data move along the diagram, we can see that they do not cross the separating line. Only one patient (ID 22) behaves differently. After checking the principal components for the case of this patient, we found that PC 4, obtained when patient 22 is left out, fits with PC 5 of the rest of cases. Therefore, we have used  $C_{4,22}$  instead of  $C_{5,22}$ . In summary, the results obtained from the application of the LOOCV method support the procedure given in this paper.

#### 4 Conclusions

In this work, a significant difference in the Raman spectra of subjects with and without nickel allergy has been obtained by means of PCA. The difference in Raman spectra can be explained by biochemical differences in the skin, which might be due to filaggrin or natural moisturizing factor deficiencies which have been linked to different types of skin allergy.<sup>1</sup> Using PCA, we could identify those spectral regions that can be of interest for the classification of the spectra. This classification has been possible when analyzing both the eigenvectors of the PCA and also the reconstructed spectra using a selected and significant subset of principal components.

Also, an alternative approach was developed for a fast evaluation and classification of the given spectra into two clinically distinct groups. It is based on the evaluation of the cosines of the angles between the spectrum under analysis and the spectra of a selected subset of principal components. These PCs have been identified after a detailed analysis of the results of the method applied to a collection of Raman spectra. This technique is mathematically simple, does not require a new PCA evaluation when classifying a new spectrum, and could be implemented for a

rapid classification. The method has been checked using a LOOCV test obtaining satisfactory results. As in any classification technique, the result benefits from a reliable database of previously measured subjects.

#### Acknowledgments

This work has been partially supported by the Mobility Program of Distinguished Researchers funded by Fundación Santander and managed by the University Complutense of Madrid. The authors also acknowledge M. G. Ramírez-Elías for assistance with the Raman spectroscopy measurements.

#### References

1. J. P. Thyssen and T. Menne, "Metal allergies: a review on exposures, penetration, genetics, prevalence, and clinical implications," *Chem. Res. Toxicol.* **23**(2), 309–318 (2010).
2. I. Marenholz et al., "Filaggrin loss-of-function mutations predispose to phenotypes involved in the atopic march," *J. Allergy Clin. Immunol.* **118**(4), 866–871 (2006).
3. D. J. Gawkrödger, C. W. McLeod, and K. Dobson, "Nickel skin levels in different occupations and an estimate of the threshold for reacting to a single open application of nickel in nickel-allergic subjects," *Br. J. Dermatol.* **166**(1), 82–87 (2012).
4. Q. Matthews et al., "Biochemical signatures of *in vitro* radiation response in human lung, breast and prostate tumour cells observed with Raman spectroscopy," *Phys. Med. Biol.* **56**(21), 6839–6855 (2011).
5. N. J. Crane and E. A. Elster, "Vibrational spectroscopy: a tool being developed for the noninvasive monitoring of wound healing," *J. Biomed. Opt.* **17**(1), 010902 (2012).
6. A. Beljebbar et al., "Identification of Raman spectroscopic markers for the characterization of normal and adenocarcinomatous colonic tissues," *Crit. Rev. Oncol. Hematol.* **72**(3), 255–264 (2009).
7. B. W. Barry, H. G. M. Edwards, and A. C. Williams, "Fourier transform Raman and infrared vibrational study of human skin: assignment of spectral bands," *J. Raman Spectrosc.* **23**(11), 641–645 (1992).
8. R. J. Swain, G. Jell, and M. M. Stevens, "Non-invasive analysis of cell cycle dynamics in single living cells with Raman micro-spectroscopy," *J. Cell. Biochem.* **104**(4), 1427–1438 (2008).
9. S. Kezic, "Methods for measuring *in-vivo* percutaneous absorption in humans," *Hum. Exp. Toxicol.* **27**(4), 289–295 (2008).
10. K. U. Schallreuter et al., "Oxybenzone oxidation following solar irradiation of skin: photoprotection versus antioxidant inactivation," *J. Invest. Dermatol.* **106**(3), 583–586 (1996).
11. M. Gniadecka et al., "Structure of water, proteins, and lipids in intact human skin, hair, and nail," *J. Invest. Dermatol.* **110**(4), 393–398 (1998).
12. M. Gniadecka et al., "Water and protein structure in photoaged and chronically aged skin," *J. Invest. Dermatol.* **111**(6), 1129–1133 (1998).
13. M. Gniadecka et al., "Melanoma diagnosis by Raman spectroscopy and neural networks: structure alterations in proteins and lipids in intact cancer tissue," *J. Invest. Dermatol.* **122**(2), 443–449 (2004).
14. S. Sigurdsson et al., "Detection of skin cancer by classification of Raman spectra," *IEEE Trans. Biomed. Eng.* **51**(10), 1784–1793 (2004).
15. F. J. González et al., "Use of Raman spectroscopy in the early detection of filaggrin-related atopic dermatitis," *Skin Res. Technol.* **17**(1), 45–50 (2011).
16. F. J. González et al., "Noninvasive detection of filaggrin gene mutations using Raman spectroscopy," *Biomed. Opt. Express* **2**(12), 3363–3366 (2011).
17. V. Mlitz et al., "Impact of filaggrin mutations on Raman spectra and biophysical properties of the stratum corneum in mild to moderate atopic dermatitis," *J. Eur. Acad. Dermatol. Venereol.* **26**(8), 983–990 (2012).
18. U. Hillen et al., "Late reactions to patch test preparations with reduced concentrations of *p*-phenylenediamine: a multicentre investigation of the German Contact Dermatitis Research Group," *Contact Dermatitis* **64**(4), 196–202 (2011).

19. J. Zhao et al., "Automated autofluorescence background subtraction algorithm for biomedical Raman spectroscopy," *Appl. Spectrosc.* **61**(11), 1225–1232 (2007).
20. I. T. Jolliffe, *Principal Component Analysis*, Springer-Verlag, New York (2002).
21. J. M. López-Alonso, J. Alda, and E. Bernabeu, "Principal characterization of noise for infrared images," *Appl. Opt.* **41**(2), 320–331 (2002).
22. M. G. Ramirez-Elias, J. Alda, and F. J. González, "Noise and artifact characterization of *in vivo* Raman spectroscopy skin measurement," *Appl. Spectrosc.* **66**(6), 650–655 (2012).
23. O. Devillers et al., "Separating several point sets in the plane," in *Proc. 13th Can. Conf. Comput. Geometry*, pp. 81–84, CCCG, Waterloo, Ontario (2001).
24. S. Geisser, *Predictive Inference: An Introduction*, Chapter 2, Chapman & Hall, New York (1993).